Global Change Biology

Global Change Biology (2012) **18**, 1000–1015, doi: 10.1111/j.1365-2486.2011.02566.x

From pattern to process: linking intrinsic water-use efficiency to drought-induced forest decline

JUAN CARLOS LINARES* and J. JULIO CAMARERO†

Área de Ecología, Universidad Pablo de Olavide, Ctra. Utrera km. 1, 41002 Sevilla, Spain, †ARAID, Instituto Pirenaico de Ecología (CSIC), Avda. Montañana 1005, 50192 Zaragoza, Spain

Abstract

The rise in atmospheric CO_2 concentrations (*Ca*) has been related to tree growth enhancement and increasing intrinsic water-use efficiency (iWUE). However, the extent that rising *Ca* has led to increased long-term iWUE and whether climate could explain deviations from expected *Ca*-induced growth enhancement are still poorly understood. The aim of this research was to use *Ca* and local climatic variability to explain changes during the 20th century in growth and tree ring and needle $\delta^{13}C$ in declining and nondeclining *Abies alba* stands from the Spanish Pyrenees, near the southern distribution limit of this species. The temporal trends of iWUE were calculated under three theoretical scenarios for the regulation of plant-gas exchange at increasing *Ca*. We tested different linear mixed-effects models by multimodel selection criteria to predict basal area increment (BAI), a proxy of tree radial growth, using these scenarios and local temperature together with precipitation data as predictors. The theoretical scenario assuming the strongest response to *Ca* explained 66–81% of the iWUE variance and 28–56% of the observed BAI variance, whereas local climatic variables together explained less than 11–21% of the BAI variance. Our results are consistent with a drought-induced limitation of the tree growth response to rising CO_2 and a decreasing rate of iWUE improvement from the 1980s onward in declining *A. alba* stands subjected to lower water availability.

Keywords: *Abies alba*, basal area increment, carbon isotope discrimination, climate warming, drought, intrinsic water-use efficiency, tree rings

Received 12 July 2011 and accepted 12 September 2011

Introduction

It is widely acknowledged that modifications in gas exchange and growth are among the primary responses of trees to the current rise in atmospheric CO_2 concentration (Körner, 2000; Huang *et al*., 2007). During the past 100 years, the CO_2 concentration in the atmosphere has increased from 300 to 380 μmol mol^{-1} (McCarroll & Loader, 2004). If rising atmospheric CO_2 levels lead to increased photosynthetic rates but transpiration rates either remain stable or decline, then intrinsic water-use efficiency (iWUE), that is, the carbon gain per unit of water lost, will be improved. On the other hand, rising CO_2 concentrations in the atmosphere are expected to exacerbate climate warming and drought severity in some xeric regions such as the Mediterranean Basin, which could fundamentally alter the composition and structure of forests through drought-induced decline and vegetation shifts (Poorter & Navas, 2003; Ferrio *et al*., 2006; Thuiller *et al*., 2008; Allen *et al*., 2010; Gonzalez *et al*., 2010; Galiano *et al*., 2011; Linares & Tíscar, 2011).

Correspondence: Juan Carlos Linares, tel. + 34 953 212 551, fax + 34 953 211 873, e-mail: jclincal@upo.es

Increased atmospheric CO_2 concentration (*Ca*) may stimulate plant growth, indirectly through reduced water consumption by plants and hence slower soil-moisture depletion, and directly through enhanced photosynthesis (Ceulemans & Mousseau, 1994; Norby *et al*., 2005). Experimental results show that plants can increase their iWUE as *Ca* levels rise (Körner *et al*., 2007). However, the extent that rising *Ca* may stimulate tree growth and whether plant acclimation to elevated CO_2 and climate change could explain deviations from the projected CO_2-induced growth enhancement are still poorly understood (Peñuelas *et al*., 2010; Gagen *et al*., 2011).

At present, knowledge concerning the long-term effects of *Ca* on tree growth is incomplete as, despite the greater atmospheric CO_2 concentrations and expected increases in iWUE during the last century, tree growth and iWUE have not risen as expected and they have remained stable or even declined in some areas, suggesting that other local stress factors have overridden the expected CO_2-induced growth increase (Poorter & Pérez-Soba, 2001; Saurer *et al*., 2004; Waterhouse *et al*., 2004; Martinez-Vilalta *et al*., 2008; Peñuelas *et al*., 2010; Andreu-Hayles *et al*., 2011). Several studies using $^{13}C/^{12}C$ isotopic ratios ($\delta^{13}C$) in annual rings from trees growing under natural

conditions worldwide show that trees vary in their responses to the increasing atmospheric CO_2 concentrations, suggesting an interaction with other changing environmental factors (Ferrio *et al*., 2006; Peñuelas *et al*., 2010; Silva *et al*., 2010; Andreu-Hayles *et al*., 2011). Climate change and particularly warming-related drought, nutrient limitation and/or physiological long-term acclimation to elevated *Ca* have been proposed as potential factors that could limit the expected CO_2 fertilization effect (Hyvönen *et al*., 2007; Levanič *et al*., 2011).

Long-term field studies, based primarily on tree rings of conifers, in the United States (Marshall & Monserud, 1996; Feng, 1998) and in northern Europe (Saurer *et al*., 2004; Waterhouse *et al*., 2004; Gagen *et al*., 2011) have revealed wide variability among forests and trees in their radial growth and iWUE responses to rising atmospheric CO_2. In most places, iWUE has been increasing, but there is a lack of understanding on why this variable has improved more at some sites than in others. Some argue for the hypothesis that greater CO_2 can offset the impact of a higher degree of stomatal closure due to increased dryness, resulting in no substantial reduction of carbon gain. However, this scenario is unlikely in water-limited forests (Peñuelas *et al*., 2008; Linares *et al*., 2009).

We assume that tree vulnerability to a given type of climate change is determined mainly by inherent drought sensitivity and adaptive capacity to local conditions and that the growth responses to changes in *Ca* and climate (here regarded as predictors) can be used as a surrogate for assessing a species' vulnerability to climate change (Ogle *et al*., 2000; Linares *et al*., 2010; Carnicer *et al*., 2011). Our approach provides a novel advance for analysing the effects of both climatic stress and intrinsic iWUE on radial growth, using linear mixed-effects models to quantify the increment in basal area at the individual level.

Here, we focus on silver fir (*Abies alba* Mill.), a drought-sensitive tree species (Bert *et al*., 1997), which has recently undergone drought-induced decline in the Spanish Pyrenees, that is, near the southern xeric distribution limit of this species (Camarero *et al*., 2011). Our starting hypothesis was that, in water-limited *A. alba* populations, drought and temperature increases affect tree growth and carbon storage in a particularly negative way, despite rising atmospheric CO_2 concentrations. To test this, we investigated 20th-century local climatic trends (temperature and precipitation), $\delta^{13}C$ changes in tree rings and needles and basal area increment (BAI; as a surrogate of radial growth and net carbon gain) in declining and nondeclining *A. alba* stands. Our specific aims were (i) to quantify the extent to which the rising atmospheric CO_2 concentrations boosted tree growth and iWUE of *A. alba* near the xeric distribution limit of the species, and (ii) to evaluate whether climate change could explain deviations from expected CO_2-induced tree growth and iWUE enhancement. The fulfilment of these aims will contribute to the understanding of the long-term links between WUE and growth in trees as well as to evaluate whether these variables are appropriate to forecast drought-induced decline.

Materials and methods

Study species and field sampling

The Pyrenees constitute a transitional area between moister conditions on their northern edge and drier conditions southwards where Mediterranean vegetation becomes dominant. The *A. alba* populations studied are located in the Aragón Pyrenees, NE Spain (Table 1), where silver fir stands are

Table 1 Geographical, topographical and structural characteristics of the sampled sites. Values are means ± SE

Site (code)	Type of site	Latitude (N)	Longitude (W)	Aspect	Elevation (m)	Slope (°)	dbh (cm)	Height (m)	Basal area (m^2 ha^{-1})
Paco Ezpela-high (PE)	Declining	42°45′	0°52′	NE	1232	27	35.0 ± 2.3	18.2 ± 0.9	10.1
Paco Ezpela-low (PZ)	Declining	42°45′	0°52′	NE	1073	26	43.0 ± 1.2	21.4 ± 0.6	24.7
Lopetón (LO)	Declining	42°46′	0°52′	NW	1009	32	38.1 ± 2.7	20.8 ± 0.8	24.8
Paco Mayor (PM)	Declining	42°42′	0°38′	N	1333	30	49.8 ± 3.3	24.0 ± 0.6	32.9
Gamueta (GA)	Nondeclining	42°53′	0°48′	NW	1400	23	64.2 ± 2.2	30.1 ± 1.1	55.8
Los Abetazos (AB)	Nondeclining	42°43′	0°33′	N	1403	20	75.0 ± 4.4	22.2 ± 0.9	63.8
Lierde (LI)	Nondeclining	42°42′	0°33′	N	1222	21	74.1 ± 4.1	27.5 ± 0.6	87.1
Izquierda del Aragón (IA)	Nondeclining	42°45′	0°31′	W	1478	27	69.0 ± 5.6	24.9 ± 0.9	56.0

usually found at moist sites on north-facing slopes, forming pure or mixed stands with *Fagus sylvatica* L. or *Pinus sylvestris* L. Most of the stands studied are located on marls and limestones, which generate basic soils, or on moraine deposits with rocky but deep soils. The most commonly used method of timber harvesting in the study area was diameter limit cutting, which affected mostly large, fast-growing trees (Cabrera, 2001). According to historical data cited by this author, logging intensity during the 20th century in the Pyrenees was greatest in the 1950s.

In the Aragón Pyrenees, silver fir growth decline characterized by severe defoliation and high mortality rates has affected mostly low-elevation sites since the 1980s (Camarero *et al.*, 2011). To compare *A. alba* stands with contrasting decline symptoms, we performed an extensive field survey, visiting 32 forests with at least one sampled site in all 10 km^2 grids where silver fir formed forests across the Aragón Pyrenees. Based on this extensive field survey, we selected four representative declining and nondeclining *A. alba* stands, respectively (Table 1; see also Figs S1 and S2). Declining trees were defined as those with crown defoliation greater than 50%, and declining sites were regarded as those where more than 25% trees had such a degree of defoliation decline. On average, declining sites showed a significantly higher frequency of dead trees (10.8 ± 1.1%) than nondeclining sites (1.9 ± 0.4%; Mann–Whitney test, $U = 7.5$, $P < 0.001$).

At each site, 10–15 dominant trees were selected for sampling within a 500 m long and 20 m wide transect randomly located within the stand. Distance between trees was always greater than 20 m. Elevation, aspect and slope steepness were measured in the field at the tree level. We measured the size of each tree located within the transect (diameter at 1.3 m from the base, dbh), and assessed their vigour using a semi-quantitative scale based on the percentage of crown defoliation (Müller & Stierlin, 1990): class 0, 0–10% defoliation (healthy tree); 1, 11–25% (slight damage); 2, 26–50% (moderate damage); 3, 51–75% (severe damage); 4, 76–90% (dying tree); 5, dead trees with >91% defoliation or only retaining red needles. As percentage estimates of crown defoliation may vary among observers and places, at each site we randomly selected five trees with maximum amount of green needles. These trees were used as reference 'healthy' trees to correct for observer bias in estimates of defoliation of similar sized trees in the study area.

Dendrochronological methods

In 10–15 randomly selected trees, dendrochronological sampling was performed at each site, following standard methods (Fritts, 1976). Two or three cores were taken from each tree at breast height (1.3 m) using an increment borer. The wood samples were air-dried and polished with a series of successively finer sand-paper grits. The samples were visually cross-dated. Tree rings were measured to the nearest 0.01 mm using a binocular scope and a LINTAB measuring device (Rinntech, Heidelberg, Germany). Cross-dating of the tree rings was checked using the program COFECHA (Holmes, 1983). The trend due to the geometrical constraint of adding a volume of wood to a stem of increasing radius was corrected by converting tree ring widths into BAIs (Biondi & Qaedan, 2008). We also calculated a percent growth reduction (GR) for the last decades of the 20th century as GR = 100 × [(mean BAI of the last decade included in the compute) − (mean BAI of the first decade included in the compute)]/(mean BAI of the first decade included in the compute).

Temporal trends of carbon discrimination and iWUE

To compare the long-term changes in iWUE of two nearby declining and nondeclining silver fir forests, we reconstructed their $^{13}C/^{12}C$ isotope ratios ($\delta^{13}C$) in wood cellulose from cross-dated annual tree rings during the 20th century and in annual needle cohorts formed from 1993 to 2002. We selected two sites with contrasting degrees of defoliation (PE, declining site; GA, nondeclining site; Table 1). The declining site (PE) was one of the most heavily affected stands, with 50% of all sampled trees showing severe defoliation, whereas no defoliation was detected at the nondeclining site (GA). The sampling and dendrochronological procedures were similar to those explained before, but an additional core per tree was taken for isotopic analyses from additional trees. The sampled trees were dominant (dbh > 20 cm, height > 10 m) and of similar size and age within each stand, being consistently older than 100 years. To avoid the juvenile effect, which produces more negative values of $\delta^{13}C$ in wood generated during the first few decades of growth (Heaton, 1999), we sampled the most recent 100 years of annual rings.

We used pooled wood (needles) samples, mixing material of the same cross-dated ring (needle cohort) from 8 to 12 different trees per site. In the study sites silver fir hold up to 15-year-old needles. Branches (2–3 per tree) were collected in late September from the upper part and southern side of the crowns. The samples were weighed on a balance (Mettler Toledo AX205, Mettler-Toledo GmbH, Zurich, Switzerland), carefully homogenized using a ultra centrifugation mill (Retsch ZM1, Retsch, Haan, Germany; mesh size of 0.5 mm; Borella *et al.*, 1998). We extracted the wood holocellulose of annual tree rings following Loader *et al.* (1997). Resin, fatty acids, ethereal oils and hemicellulose with a solution of 5% NaOH for 2 h at 60 °C were extracted repeating this procedure twice. Next, lignin was extracted with a 7% $NaClO_2$ solution for 48 h at 60 °C, and this solution was changed daily. This step was repeated until a 'white' sample as compared with commercial cellulose was obtained (Leavitt & Danzer, 1993). Finally, samples were washed 3–4 times with boiling distilled water, oven-dried (60 °C, 48 h) and weighed. Carbon isotopes were measured as CO_2 by combusting the cellulose samples in an elemental analyser attached to an isotope-ratio mass spectrometer (Thermo Finnigan MAT 251, Thermo Finnigan MAT, Bremen, Germany). The results were expressed as relative differences in $^{13}C/^{12}C$ ratio of tree material with respect to the Vienna Pee-Dee Belemnite (V-PDB) standard. Two analytical standards (cellulose, $\delta^{13}C = -24.72‰$; phthalic acid, $\delta^{13}C = -30.63‰$) were introduced every 10 samples to determine the accuracy of analyses, which was 0.07‰.

Isotopic discrimination between the carbon of atmospheric CO_2 and plant carbon (Δ; see Farquhar & Richards, 1984) in C_3 plants is a result of the preferential use of ^{12}C over ^{13}C during photosynthesis, and it is defined as follows:

$$\Delta = \frac{(\delta^{13}C_{atm} - \delta^{13}C_{plant})}{(1 + \delta^{13}C_{plant}/1000)}, \quad (1)$$

where $\delta^{13}C_{atm}$ and $\delta^{13}C_{plant}$ are the isotope ratios of carbon ($^{13}C/^{12}C$) in atmospheric CO_2 and plant material (tree rings and needles), respectively, expressed in parts per thousand (‰) relative to the standard V-PDB; Δ is linearly related to the ratio of intercellular (*Ci*) to atmospheric (*Ca*) CO_2 mole fractions, by Eqn (2) (see Farquhar *et al.*, 1982):

$$\Delta = \frac{a + (b - a)Ci}{Ca}, \quad (2)$$

where a is the fractionation during CO_2 diffusion through the stomata (4.4‰; O'Leary, 1981), and b is the fractionation associated with reactions by Rubisco and phosphoenolpyruvate carboxylase (27‰; Farquhar & Richards, 1984). *Ca* and $\delta^{13}C_{atm}$ were obtained from published data (see table 2 in McCarroll & Loader, 2004). We evaluated how ambient CO_2 partial pressure was related to elevation differences and if this might affect our iWUE estimations following Hultine & Marshall (2000). The ambient CO_2 partial pressure was estimated for each stand by multiplying the *Ca* mole fraction by total barometric pressure (BP, Pascal), estimated as:

$$BP = \frac{101.325}{e^{[(z/29.3)/T_k]}}, \quad (3)$$

where z is the altitude above sea level (m; see Table 1) and T_k is the mean May–August air temperature (K). As both elevation (1230 and 1400 m for declining and nondeclining sites, respectively) and mean May–August temperature (15.9 °C and 15.3 °C for declining and nondeclining sites, respectively) were not very different, the resulting partial CO_2 pressure was similar and showed identical long-term trends (see Supporting Information, Fig. S3). Therefore, for the sake of simplicity, we used the same *Ca* values for declining and nondeclining sites.

The *Ci*/*Ca* ratio reflects the balance between net assimilation (A) and stomatal conductance for CO_2 (g_c) according to Fick's law: $A = g_c(Ca - Ci)$. Stomatal conductances for CO_2 and water vapour (g_w) are related by a constant factor ($g_w = 1.6g_c$), and hence linking the leaf-gas exchange of carbon and water. The linear relationship between *Ci*/*Ca* and Δ [Eqn (2)] may be used to calculate the iWUE (iWUE = A/g_w), which is also defined as:

$$iWUE = \frac{Ca(b - \Delta)}{1.6(b - a)}. \quad (4)$$

The iWUE (μmol mol^{-1}), defined as the ratio of net assimilation to stomatal conductance to water vapour, was introduced to compare photosynthetic properties independently of evaporative demand and has been widely related to long-term trends in the internal regulation of carbon uptake and water loss in plants (see McCarroll & Loader, 2004; Robertson *et al.*, 2008).

Climate data

We used local climate records to study the spatio-temporal variation of climatic conditions in the study area (Table S1). We created two subregional climate records for the silver fir declining and nondeclining sites, based on the distance to sampling sites, averaging the longest and most complete local climate records available for the study area. All climatic stations were located at ca. 1–5 km from the nearest sampling site. Annual precipitation in the study area increases with elevation ($y = 2.1x + 661$; $R^2 = 0.85$, $P < 0.05$; $n = 5$), accounting for a range of total annual precipitation from 1000 mm to 1800 mm. Mean annual temperature was 10.0 °C, without significant differences for the elevation range studied (820–1160 m a.s.l.). Total seasonal precipitation and mean temperature were calculated for winter (previous December, January and February), spring (March, April and May), summer (June, July and August) and autumn (September, October and November). We used monthly climatic data (mean temperature, total precipitation) and seasonal average temperature and total precipitation as predictor variables to explain changes in BAI.

Data analyses and modelling

Temperature, precipitation, $\delta^{13}C$ of tree rings and needles, Δ, iWUE and BAI trends were calculated for different time periods by least-squares linear regression and tested for a significance level of $P < 0.05$. The differences among trends (slopes) for a given variable were assessed by the two-slope comparison test, which compares the slopes and intercepts of two regression lines (see Zar, 1999).

Theoretical scenarios of WUE

The temporal trends of Δ and iWUE were calculated under three theoretical scenarios for the regulation of plant-gas exchange fractionation during CO_2 diffusion through the stomata (see Saurer *et al.*, 2004; Seibt *et al.*, 2008). The isotope values of the tree rings are chosen to match specific gas-exchange responses, namely (i) *Ci* = constant, (ii) *Ci*/*Ca* = constant and (iii) *Ci* − *Ca* = constant. The scenarios differ in the degree to which the increase in *Ci* follows the increase in *Ca*: either (i) not at all, (ii) in a proportional way or (iii) at the same rate. Values for the atmosphere (*Ca* and $\delta^{13}Ca$) are taken from the literature as explained before, while the starting level for *Ci* in all scenarios is the average *Ci* for the sampled tree rings in the period 1900–1905 inferred from Eqn (2). In Scenario 1, *Ci* is kept constant and $\delta^{13}C$ from tree rings must therefore increase according to Eqns (1) and (2), while *Ci*/*Ca* and Δ decrease (see Supporting Information). On the other hand, *Ci* − *Ca* and iWUE increase strongly. In Scenario 2, $\delta^{13}C$ tree rings is hypothesized to decrease in parallel with $\delta^{13}C$ because of constant *Ci*/*Ca* and Δ. Accordingly, iWUE is still improved, but not as strongly as in Scenario 1, whereby *Ci* is also increasing. The situation of constant *Ci*/*Ca* and Δ reflects proportional regulation of A and g (see Supporting Information). In Scenario 3, *Ci* follows exactly the increase in *Ca* and *Ci* − *Ca* remains

constant. Here, $\delta^{13}C$ in tree rings decreases more strongly than the isotopic composition of the atmosphere and, accordingly, discrimination increases. This represents a relatively weak stomatal response and iWUE is not improved (see Supporting Information, Fig. S4). These scenarios will be used as a guideline for interpreting the observed tree ring carbon isotope values for declining and nondeclining sites.

Linear mixed-effects models explaining BAI

We considered a general framework to understand tree growth described by the following simple equation:

$$\text{Carbon gain} = \text{carbon uptake} - \text{carbon loss}. \quad (5)$$

Then, we used BAI as a surrogate of net carbon gain, assuming that secondary wood growth was correlated with the whole-tree carbon budget (e.g. Waring *et al*., 1998; Litton *et al*., 2007; McDowell *et al*., 2008, 2010). Thus, we assumed that radial growth was a reliable indicator of tree decline (Das *et al*., 2007). Indeed, several studies have reported low relative growth (Linares *et al*., 2010), negative growth trends (Bigler *et al*., 2004), higher variation in growth (Ogle *et al*., 2000) and greater sensitivity to climate (Pedersen, 1998; Suarez *et al*., 2004) as characteristic growth patterns of declining and dying trees.

From Eqn (4), we can estimate the average carbon uptake as a mean tree photosynthetic rate which depends on stomatal conductance and WUE:

$$A = \text{iWUE} g_w. \quad (6)$$

Then, the three iWUE theoretical scenarios at increased *Ca* explained before were used as predictors for BAI. We used theoretical iWUE scenarios instead of iWUE measured from tree ring $\delta^{13}C$ because the carbon isotope discrimination responds to many environmental factors besides CO_2, especially to climatic factors. Therefore, we expected that a significant amount of tree ring $\delta^{13}C$ variance (particularly high-frequency variability) would be more related to climate than to increasing atmospheric CO_2 concentrations (McCarroll & Loader, 2004; Saurer *et al*., 2004; Robertson *et al*., 2008; Peñuelas *et al*., 2010). Finally, we assumed that both the component of Eqn (4) related to stomatal conductance regulation (g_w), and the carbon loss component (related, e.g. to warming-induced respiration rates increase; Atkin *et al*., 2005), would be reflected by climate variables included in the model [see Eqn (6)].

We fitted linear mixed-effects models using the *nlme* package in R software (R Development Core Team, 2011) to explain BAI of nondeclining trees and declining trees using the three theoretical iWUE scenarios and climate as explanatory variables. iWUE and climate were included as fixed effects, and each tree was included as a random effect based on the following equation:

$$\text{BAI} = I + \text{iWUE}_{Ca} + \text{precipitation} + \text{temperature} + \varepsilon, \quad (7)$$

where I is the intercept; iWUE_{Ca} represents the different theoretical iWUE scenarios for regulation of plant-gas exchange at increased *Ca*; precipitation and temperature represent the monthly data for these two variables taken from local data; and ε is the error component (Pinheiro *et al*., 2011). The covariance parameters were estimated using the restricted maximum likelihood method, which estimates the parameters by minimizing the likelihood of residuals from the fitting of the fixed-effects portion of the model (see further details in Zuur *et al*., 2009). We used an information-theoretic approach for multimodel selection, based on the Akaike's information criterion (AIC; Akaike, 1974) corrected for small sample sizes (AICc). The AIC combines the measure of goodness of fit with a penalty term based on the number of parameters used in the model. We considered models with substantial support to be those in which the ΔAIC (i.e. the difference of AICc between models) was < 2 (see Burnham & Anderson, 2002).

Results

Climatic variability and trends

Overall, mean climatic conditions in declining sites were warmer and drier than in nondeclining sites (Table 2). The year-to-year variability also differed between both types of sites based on local climatic data. For instance, total annual precipitation and mean annual temperature varied between 638–1686 mm and 1065–2750 mm and 8.6–12.0 °C and 7.2–10.8 °C in meteorological stations near declining (Ansó) and nondeclining (Canfranc) sites, respectively (Table S1). Linear regressions showed a significant increase in mean annual temperature over the 20th century (+1.3 °C on average; Table 2), mainly due to warming trends since the 1970s. The slopes corresponding to mean annual temperature did not differ significantly between declining and nondeclining sites. Winter registered the greatest temperature rise (+1.7 °C), while spring had the lowest warming, although it has strongly increased since 1970 (Table 2 and Fig. 1a). Annual precipitation showed significant positive trends over the 20th century span at nondeclining sites (+262 mm on average; Table 2), where the greatest precipitation increase was found in winter (+112 mm). Although precipitation trends were not significant at declining sites, droughts were more severe than at nondeclining sites, particularly since the mid-1980s onwards (Fig. 1b).

Trends in carbon isotopes discrimination and WUE

At the declining site, we detected a slight decrease in the tree ring $\delta^{13}C$ of $-0.76‰$ over the 20th century. In contrast, we found a rising $\delta^{13}C$ trend that yielded a slight increase of $+0.69‰$ at the nondeclining site for the same period. These trends resulted in the convergence in tree ring $\delta^{13}C$ values between the two sites,

Table 2 Climatic and tree rings carbon isotope characteristics in nondeclining and declining *Abies alba* sites

		Nondeclining sites				Declining sites			
	Period	20th century average	20th century change	1970–2000 average	1970–2000 change	20th century average	20th century change	1970–2000 average	1970–2000 change
Temperature (°C)	Winter	2.48	1.70**	3.21	2.07**	2.83	1.66**	3.44	1.56**
	Spring	7.63	1.18**	7.92	3.11**	8.27	1.08**	8.53	2.60**
	Summer	16.73	1.20**	17.18	2.17**	17.41	1.27**	17.88	1.35**
	Autumn	9.92	1.40**	10.38	1.03	10.47	1.15**	10.86	0.68
	Annual	9.19	1.37**	9.67	2.09**	9.74	1.29**	10.18	1.55**
Precipitation (mm)	Winter	268	112**	306	31	231	46	243	−40
	Spring	341	42	357	−6	290	−1	287	−63
	Summer	281	43	307	−74	224	15	239	−72*
	Autumn	309	66*	333	91	256	37	267	32
	Annual	1199	262**	1302	43	1002	97	1036	−143**
$\delta^{13}C$ (‰)		−23.94	0.69**	−23.77	−0.65*	−23.15	−0.76**	−23.55	−1.30**
Δ (‰)		17.30	−2.06**	16.57	−0.28	16.47	−0.55**	16.34	0.40
iWUE (μmol mol^{-1})		86.44	36.76**	100.30	16.35**	93.52	24.40**	102.42	10.22**

Change values were calculated as the slope of least-squares linear regressions multiplied by the number of years included in the compute. Significance levels:
*$P < 0.05$,
**$P < 0.01$.

approaching each other in the last two decades of the past century (Fig. 1c). Indeed, during the first half of the 20th century, the tree ring $\delta^{13}C$ differed between the two sites in relation to their contrasting mean precipitation (Fig. 1b, c and Table 2).

During the first half of the past century, mean tree ring Δ values were lower at the declining (16.64 ± 0.07‰) than at the nondeclining sites (17.81 ± 0.09‰). Thereafter, between-site differences for Δ narrowed, mainly since the 1980s (Fig. 1d). On average, the 20th century change in tree ring Δ was one fourth in the declining site as compared with the nondeclining one (−0.55‰ vs. −2.06‰, respectively; Table 2 and Fig. 1d).

During the 20th century, the iWUE of the declining site increased 0.22 μmol mol^{-1} per year, while at the nondeclining site this positive rate (0.35 μmol mol^{-1} per year) was significantly higher ($P < 0.05$, two-slope comparison test; see also Table 2). At both sites, the iWUE trends were significantly related to the constant *Ci* scenario (the scenario assuming the strongest response to atmospheric CO_2 concentration), which accounted for 65.7% and 81.3% of the iWUE variance at the declining and nondeclining sites, respectively (Fig. 2). However, iWUE values for the declining site were consistently lower than those predicted under a constant *Ci* scenario, since the onset of the decline in the 1980s. Indeed, the constant *Ci*/*Ca* scenario received similar support based on the AIC criterion (data not shown).

The results for needle $\delta^{13}C$ differed slightly from those for the tree rings. Mean values for needle $\delta^{13}C$ were on average more negative (about −27.5‰) than those for the same period in tree ring $\delta^{13}C$ (about −24.0‰). Therefore, the estimated mean Δ and iWUE values were lower in needle than in tree ring $\delta^{13}C$ (Figs 1–3). At the declining site, we found a slight increase in the needle $\delta^{13}C$ of +1.2‰ from 1993 to 2002, whereas tree ring $\delta^{13}C$ decreased −0.9‰ through the same period. As a result, iWUE increased for needles (+18.8 μmol mol^{-1}; $P < 0.01$) but showed nonsignificant trends for tree ring $\delta^{13}C$. In contrast, the nondeclining site showed a slight decrease in both needle and tree ring $\delta^{13}C$, with nonsignificant trends for Δ and iWUE (Fig. 3).

Relationships between climate, WUE and BAI

The quotient *Ci*/*Ca* (used as an indicator of carbon uptake per unit of atmospheric CO_2 increase) was significantly related to total annual precipitation for both declining and nondeclining sites (Fig. 4). However, this relationship was, as expected, positive (higher WUE as total annual precipitation decreases) at the declining site, but negative at the nondeclining site (higher WUE as precipitation increases). Mean annual temperature

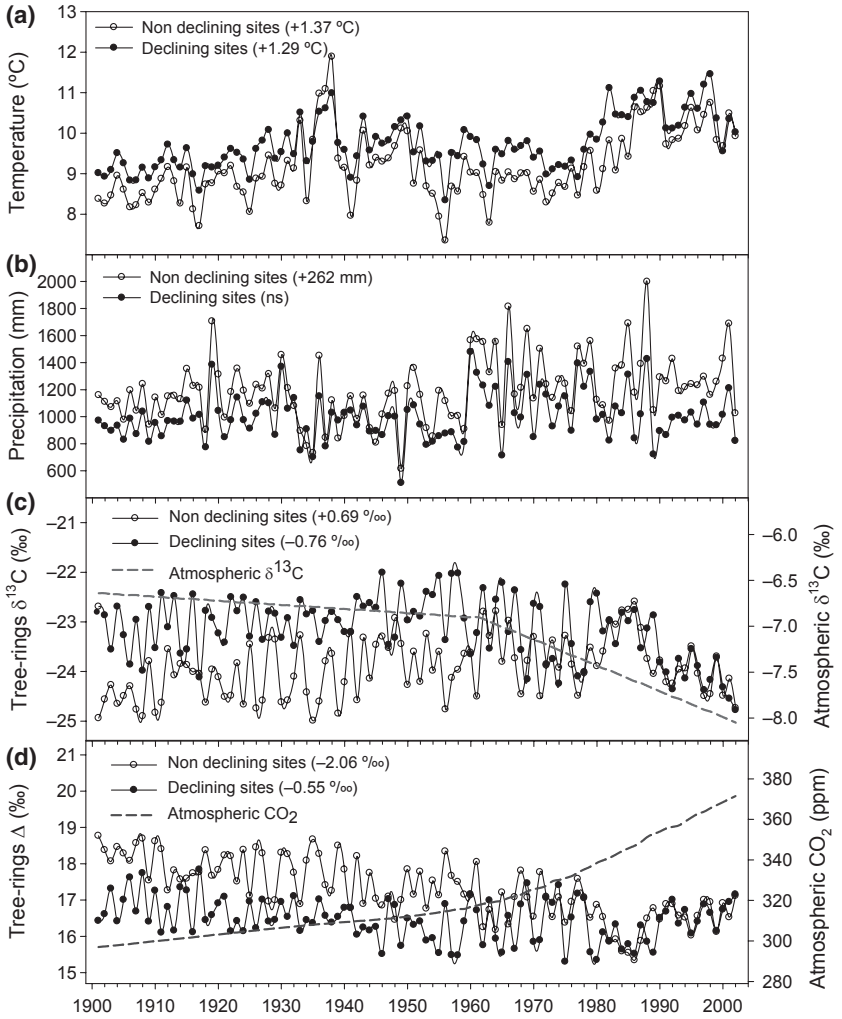

Fig. 1 Mean annual temperature (a), annual total precipitation (b), tree ring $\delta^{13}C$ (c) and Δ (d) in declining and nondeclining *Abies alba* sites from the Spanish Pyrenees. Changes in the global atmospheric CO_2 concentration and atmospheric $\delta^{13}C$ are also shown (data from McCarroll & Loader, 2004). Significant ($P < 0.05$) 20th-century changes for each variable, calculated as the linear slope of the corresponding time series multiplied by the number of years included in the compute appear within brackets.

was also significantly but negatively correlated to *Ci/Ca*, both for declining and nondeclining sites, that is, WUE increased as mean annual temperature rose. Nevertheless, the strongest relationship was obtained between *Ci/Ca* and mean BAI for nondeclining trees (Fig. 4), which indicates a significant link between WUE and growth.

More than 50% of trees from declining sites had a mean BAI lower than 15 cm^2 $year^{-1}$ during the period 1990–1999, while this occurred in 23% of trees from nondeclining sites (Fig. 5a). Moreover, severely defoliated trees (about 38% of studied trees at declining sites), showed the lowest mean BAI for the period 1990–1999 (Fig. 5b), supporting a negative association between silver fir mean BAI and defoliation in the study area (Fig. 5c).

Modelling BAI as a function of WUE and climate

Based on the results presented before, linear mixed-effects models were performed independently for trees belonging to the following defoliation percentage classes: (i) 0–25%, (ii) 26–50% and (iii) 51–100%. For these three groups, the models including iWUE as explaining variable registered the highest support (see ΔAICc in Table 3 and relative weights of variables in Table 4), while we did not find substantial support for models that included only climate variables, as compared with those that included only iWUE or both iWUE and climate as predictors (Table 3).

The model selected as the most likely to explain the BAI variability of trees belonging to 0–25% defoliation included a positive effect of iWUE, predicted under the

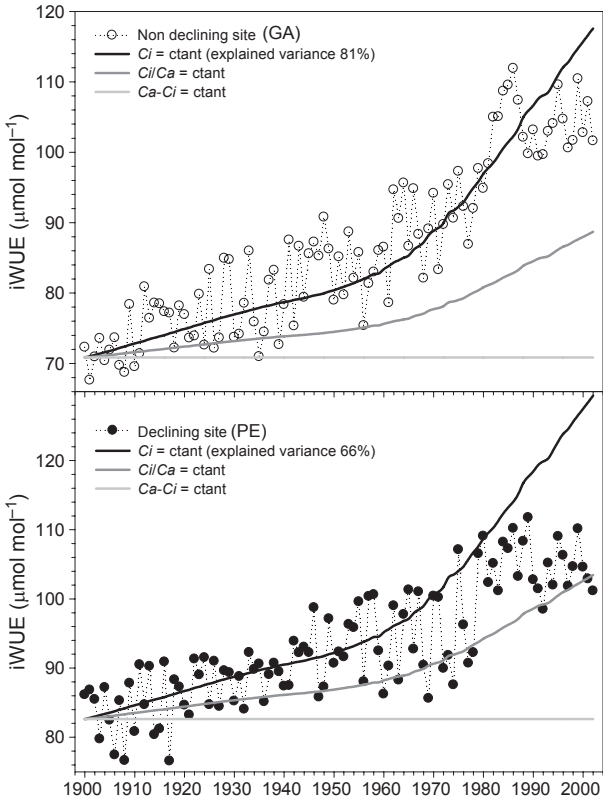

Fig. 2 Observed and theoretic changes in intrinsic water-use efficiency (iWUE) in a nondeclining site (site GA) and a declining site (site PE) representing contrasting silver fir forests from the Spanish Pyrenees. We calculated iWUE using Eqn (4), assuming three scenarios for the theoretical regulation of plant-gas exchange at an increasing atmospheric CO_2 mole fraction (*Ca*) to achieve the following: (i) a constant intercellular CO_2 mole fraction (*Ca*), (ii) a constant *Ci*/*Ca* and (iii) a constant *Ca* − *Ci*. These theoretical scenarios were compared with iWUE values taken from the tree ring $\delta^{13}C$ in trees from a declining site (PE) and a nondeclining site (GA) from the Spanish Pyrenees. The variance explained by the best-supported model (%) is also noted.

constant *Ci* scenario ($iWUE_{Ci}$, i.e. the strongest iWUE increase related to CO_2 rise) and June precipitation; and a negative effect of mean temperatures of the previous September and December as well as the current June (Tables 3 and 4). This model accounted for 57% of the BAI variance, and the higher relative weight was reached by the $iWUE_{Ci}$ (37% of the variance), followed by June mean temperature (ca. 11%).

For trees with 26–50% defoliation the model with highest support included a positive effect of $iWUE_{Ci/Ca}$ (i.e. positive iWUE response to CO_2 rise, but to a lower degree than in the constant *Ci* scenario), precipitation of the previous August and the current June; and a negative effect of mean temperatures of the previous September and the current June on growth. The model accounted for 67.15% of the variance; the highest relative weight was achieved by the $iWUE_{Ci/Ca}$ (55.81% of the variance) followed by the negative effect of current June mean temperature (5.49% of the variance).

Trees with the highest defoliation (51–100% class) yielded as the model with highest support a positive effect of $iWUE_{Ci/Ca}$ (the same as those obtained for 26–50% defoliation class), and precipitation of the current June; and a negative effect of mean temperatures of the previous August and the current May on growth. The model accounted for 41.48% of the variance; the highest relative weight was again achieved by the $iWUE_{Ci/Ca}$ (27.68% of the variance; i.e. the lowest one of the three groups) followed by the negative effect of current May mean temperature (5.40% of the variance). A model including, in addition to the aforelisted variables, a positive effect of precipitation of the previous August and a negative effect of mean temperatures of the previous December (Table 3), also received substantial support. Moreover, this second selected model, but using iWUE predicted under the constant *Ci* scenario ($iWUE_{Ci}$), also received substantial support.

Mean BAI was significantly higher at nondeclining than at declining sites over the entire study period (Fig. 6). For the period 1970–1999, the percentage of growth reduction was significantly more pronounced for declining (40%; Table 5) than for nondeclining trees (−8 to −13% on average). For the period 1980–1999, the highest growth reduction was again found for declining trees (35%), as well as the highest coefficient of variation (25%). Nondeclining trees from declining sites yielded the lowest growth reduction, while nondeclining trees from nondeclining sites showed a 7% growth reduction over the period 1980–1999.

Discussion

Deviations from the expected CO_2-induced enhancement in growth and WUE

We hypothesized that, despite that rising atmospheric CO_2 concentrations (*Ca*) could enhance growth in *A. alba*, worsening drought and rising temperatures might offset or even reverse the predicted growth enhancement in water-constrained forests. Such deviations from the expected *Ca*-induced growth enhancement (see BAI models in Table 4) provide valuable information to understand the underlying ecophysiological mechanisms leading to tree growth decline and mortality. Our results support that rising atmospheric CO_2 concentrations are linked to improved *A. alba* growth and iWUE during most of the 20th century, but from the 1980s onwards temperature warming and to a

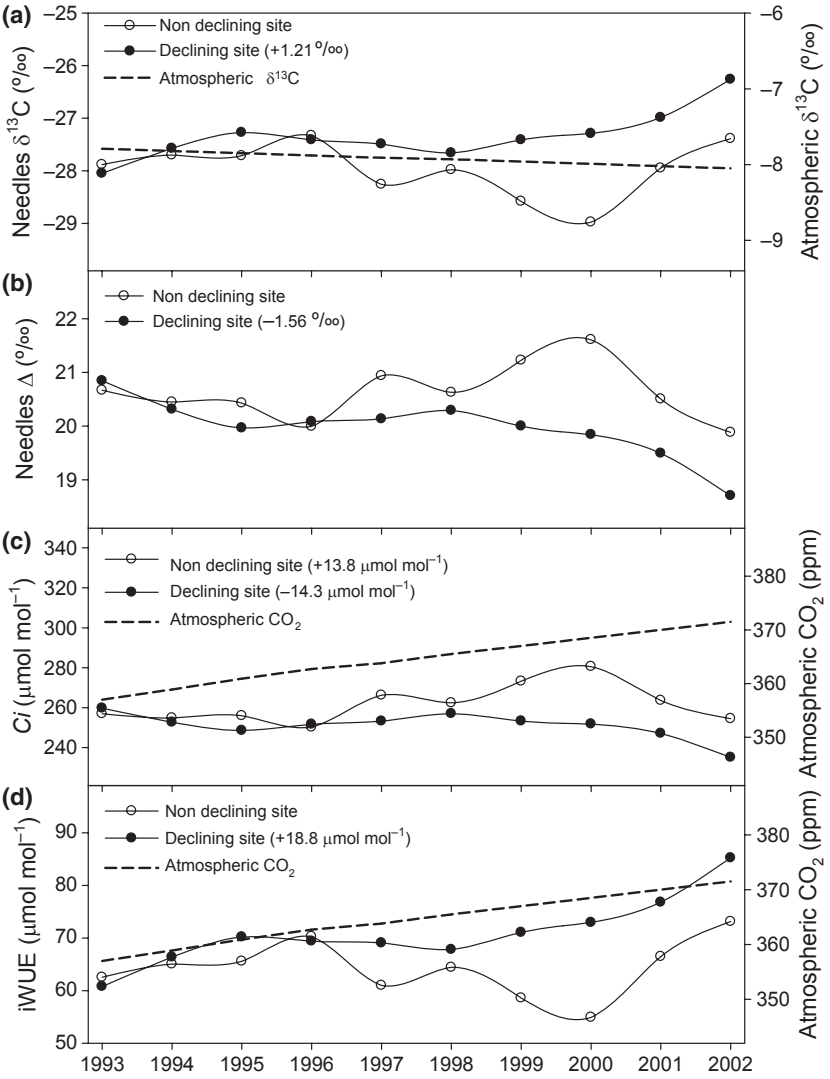

Fig. 3 Mean needle $\delta^{13}C$ (a), needle Δ (b), intercellular CO_2 mole fractions [*Ci*; (c)] and intrinsic water-use efficiency [iWUE; (d)], for a nondeclining site (site GA) and a declining site (site PE) . Changes in the global atmospheric CO_2 concentration and atmospheric $\delta^{13}C$ (data from McCarroll & Loader, 2004) are also shown. Significant ($P < 0.05$) 1993–2002 changes for each variable, calculated as the slope of the time series multiplied by the number of years included in the compute, appear within brackets.

lesser extent precipitation variability seem to have prevented the expected CO_2-induced growth stimulation.

Since the 1980s, the rate of iWUE improvement has fallen in the declining stand and stopped despite the rising atmospheric CO_2 trend. Although the reason for this decoupling is not well understood, our data show a good agreement between its timing (starting point ca. 1980), and that of the regional rise of air temperature, the succession of severe drought events, and the decline of radial growth. In Pyrenean silver fir forests drought stress may be constraining the expected growth enhancement and the predicted iWUE improvement. The combined evidence suggests that a threshold may exist in adaptive capacity of the trees to face drought as some researchers have previously reported (see, e.g. Peñuelas *et al*., 2008; Carnicer *et al*., 2011).

The increase in the iWUE found here for *A. alba* over the second half of the 20th century (ca. 27% and 11% in the declining and nondeclining sites, respectively; see Fig. 2) is within the range of iWUE values published for other forests, where an improvement in iWUE has been prevalent during the past century (Bert *et al*., 1997; Duquesnay *et al*., 1998; Feng, 1998; Saurer *et al*., 2004; Koutavas, 2008; Peñuelas *et al*., 2010). Nevertheless, some studies have found a progressively diminishing response to increasing atmospheric CO_2 concentrations (Waterhouse *et al*., 2004; Peñuelas *et al*., 2008; Linares *et al*., 2009; Andreu-Hayles *et al*., 2011;

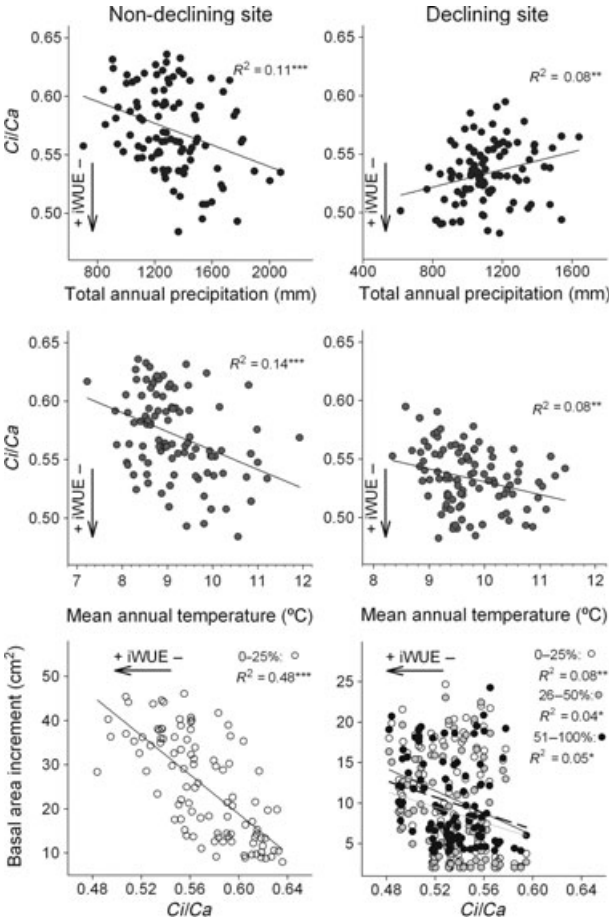

Fig. 4 Carbon uptake per unit of atmospheric CO_2 increase, expressed as the quotient between intracellular CO_2 and ambient CO_2 concentrations (Ci/Ca) vs. total annual precipitation, mean annual temperature and mean basal area increment (BAI), measured in a nondeclining *Abies alba* site (site GA) and a declining one (site PE). The inset displays the variance explained (R^2) by least-squares linear regression, as well as the Ci/Ca values indicating higher intrinsic water-use efficiency (−iWUE+, arrows). Ci/Ca vs. BAI regressions were performed separately for trees showing 0–25% crown defoliation (empty symbols; black regression line); 51–75% crown defoliation (grey symbols; grey regression line); and 76–100% crown defoliation (black symbols; dotted black regression line). $*P < 0.05$, $**P < 0.01$, $***P < 0.001$.

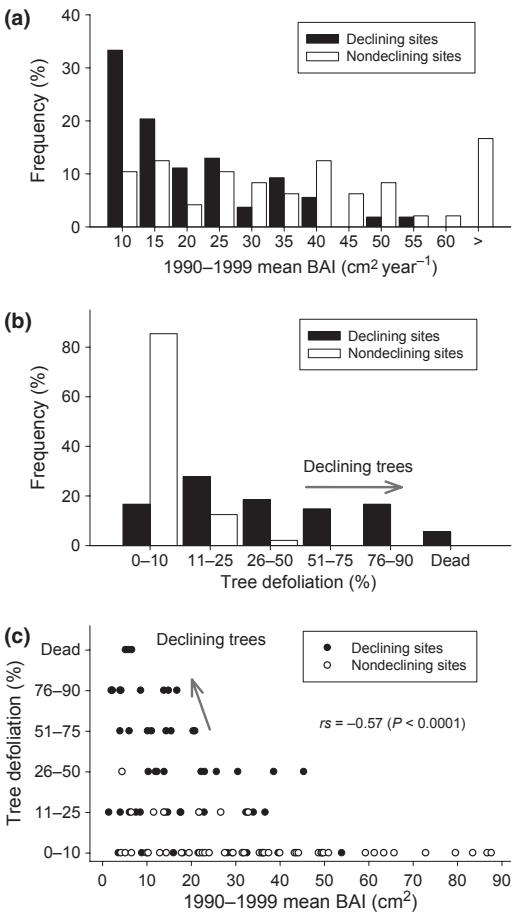

Fig. 5 Distribution frequencies of mean 1990–1999 basal area increment [BAI, (a)], tree defoliation percentage (b) and the relationship between the two variables (c) determined in declining and nondeclining *Abies alba* sites from the Spanish Pyrenees. The Spearman's correlation coefficient (rs) and related significance level (P) between the two variables are also noted. The arrows indicate the threshold for declining trees (trees showing more than 50% crown defoliation).

Gagen *et al.*, 2011), as we also report here for the declining *A. alba* forest. These forests may have reached a physiological threshold in its ability to increase iWUE as CO_2 rises due to drought-induced stomatal closure (Linares *et al.*, 2009). In contrast, the changes in iWUE of the nondeclining *A. alba* site were well represented by the theoretical scenario of a constant Ci (Fig. 2), implying a particularly strong improvement of iWUE that has not been reported elsewhere (see Peñuelas *et al.*, 2010 and references therein).

The results from needles and corresponding tree ring $\delta^{13}C$ revealed an average difference of 3–4‰, with the tree ring wood being isotopically heavier (having a less negative $\delta^{13}C$ value) than needles in agreement with other studies (Jäggi *et al.*, 2002). Despite the carbon isotopic signal in current-year needles is to some extent transferred to tree ring earlywood, postphotosynthetic mixing of different carbon pools and increased concentration of carbon components with a more negative $\delta^{13}C$ signature in the needles (e.g. lipids) modify this signal. However, we failed to find a close correspondence between the trends of $\delta^{13}C$ values in annually formed tree rings and needles (Figs 2 and 3), in agreement with other studies that yielded no significant correlations between carbon isotope discrimination of

Table 3 Model selection criteria for basal area increment (BAI) in the declining and nondeclining *Abies alba* sites. The effects of intrinsic water-use efficiency (iWUE) and climate–growth relationships were tested. A null model considering BAI as a constant (see Biondi & Qaedan, 2008) was also tested

Defoliation percentage	Model (variables)	*k*	AICc	Δ*i*	*L*(*gi*/*x*)
0–25%; 70 trees (*n* = 5489)	**iWUE$_{Ci}$ + Pjn + Tsp + Tdp + Tjn**	**7**	**44 410.06**	**0.00**	**1.00**
	iWUE$_{Ci}$ + Pjn + Pjl + Tjlp + Tsp + Tdp + Tja + Tjn + Tjl	11	44 440.32	30.26	0.00
	iWUE$_{Ci/Ca}$ + Pjn + Tsp + Tdp + Tjn	7	44 453.08	43.02	0.00
	iWUE$_{Ci/Ca}$ + Pjn + Pjl + Tjlp + Tsp + Tdp + Tja + Tjn + Tjl	11	44483.00	72.94	0.00
	iWUE$_{Ci}$	3	44 529.53	119.47	0.00
	iWUE$_{Ci/Ca}$	3	44 567.20	157.14	0.00
	Pjn + Pjl + Tjlp + Tsp + Tdp + Tja + Tjn + Tjl	10	45012.77	602.71	0.00
	iWUE$_{Ci-Ca}$	2	45 298.10	888.04	0.00
26–50%; 18 trees (*n* = 1497)	**iWUE$_{Ci/Ca}$ + Paup + Pjn + Tsp + Tjn**	**7**	**9406.97**	**0.00**	**1.00**
	iWUE$_{Ci/Ca}$ + Paup + Pjn + Pjl + Tjlp + Tsp + Tdp + Tjn + Tjl	11	9425.55	18.57	0.00
	iWUE$_{Ci}$ + Paup + Pjn + Tsp + Tjn	7	9425.47	18.50	0.00
	iWUE$_{Ci}$ + Paup + Pjn + Pjl + Tjlp + Tsp + Tdp + Tjn + Tjl	11	9444.87	37.90	0.00
	iWUE$_{Ci/Ca}$	3	9465.91	58.94	0.00
	iWUE$_{Ci}$	3	9481.90	74.93	0.00
	Paup + Pjn + Pjl + Tjlp + Tsp + Tdp + Tjn + Tjl	10	9974.60	567.62	0.00
	iWUE$_{Ci-Ca}$	2	10 185.82	778.84	0.00
51–100%; 18 trees (*n* = 1830)	**iWUE$_{Ci/Ca}$ + Pjn + Taup + Tmy**	**6**	**12 214.83**	**0.00**	**1.00**
	iWUE$_{Ci/Ca}$ + Paup + Pjn + Taup + Tdp + Tmy	**8**	**12 215.01**	**0.18**	**0.91**
	iWUE$_{Ci}$ + Paup + Pjn + Taup + Tdp + Tmy	**8**	**12 216.57**	**1.74**	**0.42**
	iWUE$_{Ci}$ + Paup + Pjn + Taup + Tmy	7	12 221.24	6.42	0.04
	iWUE$_{Ci/Ca}$	3	12 375.79	160.97	0.00
	iWUE$_{Ci}$	3	12 377.32	162.50	0.00
	Paup + Pjn + Tjlp + Taup + Tdp + Tmy + Tjl	9	12 491.77	276.94	0.00
	iWUE$_{Ci-Ca}$	2	12 706.76	491.93	0.00

k, number of parameters included in the model: the number of explaining variables plus one constant plus the error; Δ*i*, difference in AICc (Akaike information criterion corrected for small samples) with respect to the best model; *L*(*gi*/*x*), likelihood of a model *gi* given the data *x*. Values in bold correspond to models with substantial support. (+)/(−) denote positive/negative effect for variables: iWUE$_{Ci}$, intrinsic water-use efficiency [see Eqn (4)] predicted under a constant *Ci* scenario (+); iWUE$_{Ci/Ca}$, intrinsic water-use efficiency predicted under a constant *Ci*/*Ca* scenario (+); Paup, previous August precipitation (+); Pjn, June precipitation (+); Pjl, July precipitation (+); Taup, previous August temperature (−); Tsp, previous September temperature (−); Tdp, previous December temperature (+); Tja, January temperature (+); Tmy, May temperature (−); Tjn, June temperature (−); Tau, August temperature (−).

wood and needles (Leavitt & Long, 1982, 1986). This result may reflect complex interactions of differential photosynthetic efficiency of young and old needles receiving contrasting radiation intensities, which may subsequently propagate to the tree rings (Francey, 1986). Furthermore, such differences in wood and needle $\delta^{13}C$ suggest that caution should be taken regarding inferences on iWUE of trees based solely on one of these two biomass fractions.

The correlation between BAIs and the modelled iWUE was stronger than any relationship with climatic variables (Tables 3 and 4), illustrating the importance of the atmospheric CO_2 and iWUE as modulating factors of tree response to climate change (Ceulemans & Mousseau, 1994; Norby *et al*., 2005; Körner *et al*., 2007; Niinemets *et al*., 2011). Our analytical approach for the partitioning of growth variance among contributing factors showed that the responses of BAI were within the range of changes represented both by the constant *Ci* and the constant *Ci*/*Ca* scenarios (Table 3). Saurer *et al.* (2004) reported that the isotopic responses of conifers in northern Eurasia over the past century were best represented by constant *Ci*/*Ca* values, corresponding to a proportional regulation of *A* and *g*. If this is the case for *A. alba* growth, it would mean that there was a slightly lower increase in BAI than that calculated for iWUE from the isotopic data (Fig. 2).

Long tree ring chronologies revealed that the most pronounced iWUE changes were observed during the second half of the 20th century (Waterhouse *et al*., 2004; Andreu-Hayles *et al*., 2011; Gagen *et al*., 2011), but tree responses differed between stands. Overall, these studies found stronger correlations with temperature during the growing season, demonstrating that the physiological response to *Ca* changes is modulated by global warming. Since 1970, higher wood $\delta^{13}C$ values revealed

Table 4 Regression coefficients of the best-supported linear mixed-effects model explaining basal area increment (see also Table 3). For each variable, the relative weight in the model (%) and the variance explained (%) are also noted. Variables not selected (ns) in the model are also indicated

Defoliation percentage:	0–25%			26–50%			51–100%		
Independent variable	Regression coefficient	Relative weight in the model (%)	Variance explained (%)	Regression coefficient	Relative weight in the model (%)	Variance explained (%)	Regression coefficient	Relative weight in the model (%)	Variance explained (%)
$iWUE_{Ci}$	0.50	64.09	36.47	ns	ns	ns	ns	ns	ns
$iWUE_{Ci/Ca}$	ns	ns	ns	0.88	83.11	55.81	0.68	66.74	27.68
Previous August precipitation	ns	ns	ns	0.01	0.60	0.40	ns	ns	ns
June precipitation	0.02	2.64	1.50	0.02	1.55	1.04	0.03	2.54	1.05
Previous August temperature	ns	ns	ns	ns	ns	ns	−0.86	17.71	7.35
Previous September temperature	−0.65	13.17	7.50	−0.40	6.55	4.40	ns	ns	ns
Previous December temperature	−0.37	1.43	0.82	ns	ns	ns	ns	ns	ns
May temperature	ns	ns	ns	ns	ns	ns	−1.02	13.01	5.40
June temperature	−0.92	18.66	10.62	−0.51	8.18	5.49	ns	ns	ns
Total variance explained (%)	56.91			67.15			41.48		

iWUE improvements at several sites, however, water-limited forests showed iWUE values below that expected by an active response to the *Ca* increase alone (Waterhouse *et al*., 2004; Peñuelas *et al*., 2008; Linares *et al*., 2009). These patterns were related to rising temperature trends, indicating that other factors may be affecting stomatal closure in these forests. Declining growth rates during the second half of the 20th century as compared with previous centuries were also observed in long tree ring chronologies, thus providing no evidence for a recent CO_2 fertilization effect on growth.

Mechanisms underlying the decoupling between the CO_2 rise and the patterns of BAI and WUE

It should be pointed out that, despite that the rise in atmospheric CO_2 was similar in all the stands studied, as indicated by the observed positive effect of *Ca* on growth, a decoupling between the CO_2 increase and the iWUE and BAI patterns was evident from the 1970s onwards (Figs 1, 2 and 4). Such decoupling raises the issue that other factors beside CO_2 might interfere with and prevent any CO_2-induced growth stimulation. The growth variance not accounted for by iWUE was weakly related to the precipitation of the previous August and current June, which could be related to growth sensitivity to high-frequency precipitation variability (Bigler *et al*., 2004; Macias *et al*., 2006; Carnicer *et al*., 2011), as we modelled the low frequency of iWUE variability. Overall, the obtained relationships for precipitation variables were weak (Fig. 4; Tables 3 and 4), perhaps because the studied *A. alba* forest is located in mesic sites and not strongly water-limited (Fig. 1). Similar results have been obtained, for instance, in *Abies pinsapo* and *Pinus nigra* stands located at high-elevation moist sites which showed weak relationships with precipitation (Linares *et al*., 2009; Linares & Tíscar, 2011). However, our results support the hypothesis that the temperature warming is the most significant factor preventing CO_2-induced growth stimulation (Table 4).

We found a negative association between secondary growth and May–June temperature, the period when maximum radial growth rates normally take place in silver fir (Tardif *et al*., 2003; Carrer *et al*., 2010). In addition, the negative effect observed for prior August–September temperature could be related to a higher stomatal control of water loss in late summer to early autumn of the year before tree ring formation, which may reduce photosynthesis and carbohydrate synthesis as well as allocation to the stem and further secondary growth during the following spring (McDowell *et al*., 2008).

If trees react with severe stomatal closure to an earlier onset of the summer dry period, it implies a possible reduction in carbon gain despite increasing *Ca* (Körner

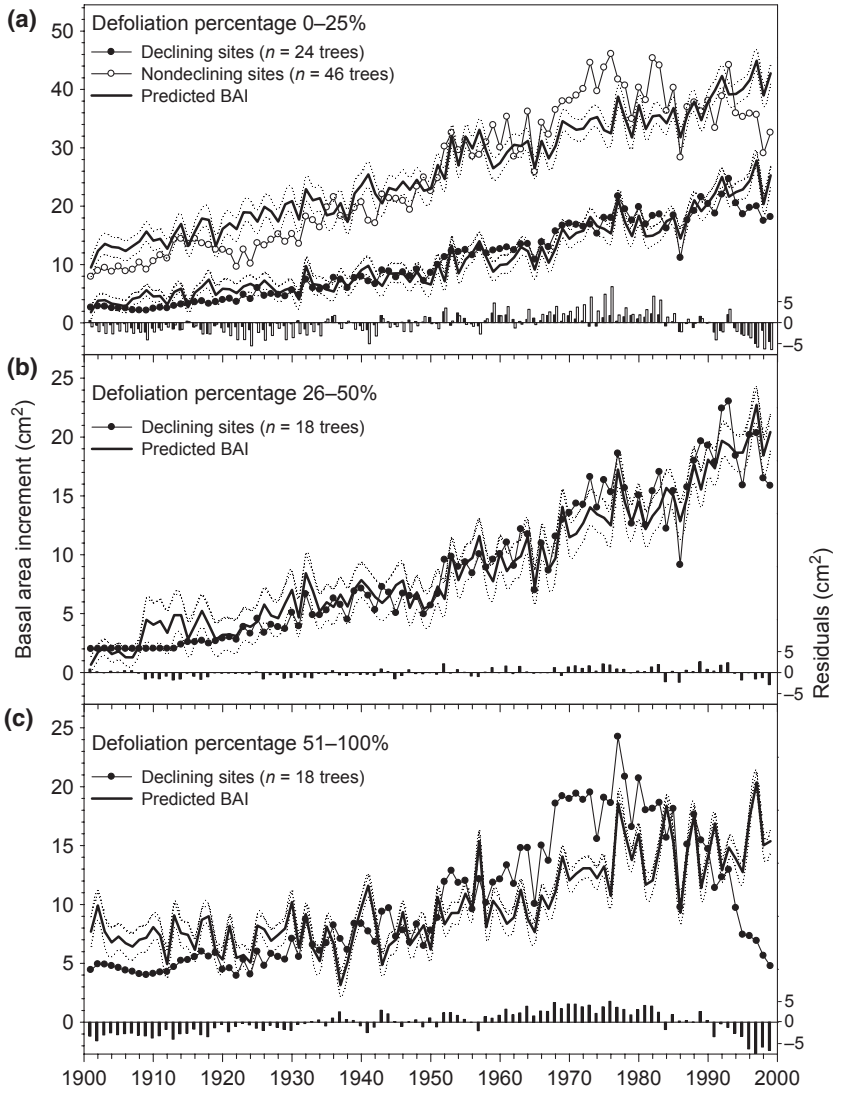

Fig. 6 Basal area increment (BAI; scatters and narrow lines) measured in trees from declining and nondeclining *Abies alba* Pyrenean sites showing different defoliation degrees: (a) 0–25% crown defoliation; (b) 26–50% crown defoliation; (c) and 51–100% crown defoliation. Linear mixed-effect model (thick lines) fits are based on intrinsic water-use efficiency and climatic variables (see also Tables 3 and 4). The bottom bar diagram represents the residuals of the linear mixed-effects model, expressed as the difference between observed minus predicted BAIs. Nondeclining sites only showed enough number of trees within the first defoliation class (a). Dotted thin lines represent the standard error.

et al., 2007; McDowell *et al*., 2008, 2010). A low availability of carbon for growth may be reflected by decreased radial growth and BAI at the declining *A. alba* site. However, the slopes of the temporal trends in BAI were similar within each stand, but dependent on the degree of defoliation undergone by trees (Figs 5 and 6). This calls into question our initial hypotheses that differing climate stress and iWUE trends might alter tree growth sensitivity to increases in CO_2. On the other hand, it supports the idea that a higher water limitation at the stand level may act as an important constraint on the adaptive capacity of drought-sensitive forests to climatic warming (McDowell *et al*., 2010; Sala *et al*., 2010; Andreu-Hayles *et al*., 2011; Levanič *et al*., 2011).

A loss of adaptive capacity can arise from the effects of drought constraining trees from fully expressing the growth potential represented by the higher CO_2 concentrations. Hence, in drought-prone forests the rate of carbon sequestration may not increase with rising atmospheric CO_2 as is often assumed by biospheric models and short-term experiments subjecting trees to elevated CO_2 concentrations (Nowak *et al*., 2004; Sitch *et al*., 2008). The failure to model a strong CO_2 fertilization effect results in the switch of the terrestrial bio-

Table 5 Mean basal area increment (BAI) values and trends in the three tree types defined in the study

	Nondeclining sites		Declining sites			
	Defoliation < 50%		Defoliation < 50%		Defoliation > 50%	
20th century mean BAI (cm^2)	24.92	b	9.80	a	9.10	a
1970–1999 mean BAI (cm^2)	37.83	b	16.75	a	14.52	a
1970–1999 trend (cm^2 $year^{-1}$)	−0.29	**a	−0.08	*b	−0.33	**a
1970–1999 growth reduction (%)	−13.05	b	−7.52	c	−39.39	a
1970–1999 coefficient of variation (%)	11.79	b	13.80	b	22.77	a
1980–1999 mean BAI (cm^2)	36.50	c	16.40	b	13.19	a
1980–1999 trend (cm^2 $year^{-1}$)	−0.38	**b	−0.12	*c	−0.55	**a
1980–1999 growth reduction (%)	−6.84	b	−3.23	c	−34.75	a
1980–1999 coefficient of variation (%)	12.07	b	15.15	b	25.07	a

Units appear within brackets. Trends are calculated as the slope of the time series, estimated by least-squares regression:
$^{*}P < 0.05$,
$^{**}P < 0.01$.
Growth reduction is calculated as: GR = 100 × [(mean BAI of the last decade included in the compute) − (mean BAI of the first decade included in the compute)]/(mean BAI of the first decade included in the compute). The coefficient of variation is defined as the ratio of the standard deviation to the mean. Different letters indicate significant differences ($P < 0.05$) for one-way ANOVAs.

sphere from a carbon sink to a net carbon source because of greater heterotrophic respiration under the concomitant effect of warming (Atkin *et al*., 2005).

Drought-induced growth decline, defoliation and trends of WUE

Our demonstration that average growth is mainly site-specific provides information that is useful for predicting stand-level decline and drought-induced mortality (Camarero *et al*., 2011). Nondeclining *A. alba* stands are at higher elevation and shallower slopes than declining stands, which should be important in terms of soil water recharge, surface evaporation and air temperature (Fig. 1 and Table 1). Climatic variability among sites was also notable as in August, the warmest and driest month in the study area, Peguero-Pina *et al*. (2007) found that air temperature ranged at 7.0–29.9 °C and 4.6–24.4 °C at declining and nondeclining stands, respectively. These authors also found that summer relative air humidity is lower in declining stands. Our results imply that trees that are already undergoing long-term water limitation, as measured by low levels of radial growth, are growing close to their lower survival threshold, and they are likely to have higher probabilities of decline and mortality when challenged with additional short-term drought stress than would trees from wetter sites (Poorter & Navas, 2003; Linares *et al*., 2010; Linares & Tíscar, 2011).

Moreover, within the drier xeric sites, the BAI of declining trees decreased in concert with the regional warming trend, while nondeclining trees from these sites showed a much less severe growth decline (Fig. 6). It should be noted that these trees represent the remaining individuals of declining stands and might undergo improved growth conditions after selective tree mortality and stand density reduction following the severe droughts of the 1980s (Camarero *et al*., 2011). This drought-induced self-thinning might enhance water, nutrient and light availability by reducing tree-to-tree competition.

In summary, our results suggest that silver fir may not be able to mitigate warming-induced growth decline by raising iWUE. The expected increase of WUE in response to rising CO_2 and drought may be achieved by greater carbon uptake, by reduced stomatal conductance or by both effects [Eqn (4); Wullschleger *et al*., 2002]. However, if drought-induced stomatal closure is too severe, it may also constrain the photosynthesis rate and subsequently tree growth. Our findings emphasize the links between tree defoliation, WUE and growth sensitivity to warming-induced drought stress. We suggest that increasing WUE and growth sensitivity to rising air temperatures will likely portray widespread and severe, in terms of defoliation and mortality, decline episodes in drought-prone areas under a warmer climatic scenario.

Conclusions

Our key finding is that WUE operates as a strong modulator of the adaptation capacity of silver fir growth in response to both long- and short-term climatic stressors. This result provides an understanding of growth

decline processes regarding not only regional climatic trends but also the inherent adaptive capacity of species to face drought by augmenting iWUE. It also highlights that iWUE should be incorporated into a conceptual framework for assessing the vulnerability of forest ecosystems to climate change, particularly in drought-prone regions. Finally, tree defoliation and mortality might be viewed in terms of short-term damage and vigour loss caused by drought, which, in the case of trees with low growth rates is more likely to result in the surpassing of physiological tolerance thresholds and the triggering decline.

Acknowledgements

This study was funded by project RTA01-071-C3-1 (INIA, Spain) and Gobierno de Aragón. The authors thank E. Martin, J. L. Vázquez, C. Lastanao and M. A. Pascual for their help. They also thank J. A. Carreira and two anonymous reviewers for their helpful comments and discussions. J. J. C. acknowledges the support of ARAID. They thank AEMET for providing climatic data. This work is humbly dedicated to Blanquita and Ceci.

References

Akaike H (1974) A new look at statistical model identification. *IEEE Transactions on Automatic Control*, **19**, 716–722.

Allen CD, Macalady AK, Chenchouni H *et al.* (2010) A global overview of drought and heat-induced tree mortality reveals emerging climate change risks for forests. *Forest Ecology and Management*, **259**, 660–684.

Andreu-Hayles L, Planells O, Gutiérrez E, Muntan E, Helle G, Anchukaitis KJ, Schleser GH (2011) Long tree-ring chronologies reveal 20th century increases in water-use efficiency but no enhancement of tree growth at five Iberian pine forests. *Global Change Biology*, **17**, 2095–2112.

Atkin OK, Bruhn D, Hurry VM, Tjoelker MG (2005) The hot and the cold: unravelling the variable response of plant respiration to temperature. *Functional Plant Biology*, **32**, 87–105.

Bert D, Leavitt SW, Dupouey JL (1997) Variations of wood $\delta^{13}C$ and water-use efficiency of *Abies alba* during the last century. *Ecology*, **78**, 1588–1596.

Bigler CJ, Gricar J, Bugmann H, Cufar K (2004) Growth patterns as indicators of impending tree death in silver fir. *Forest Ecology and Management*, **199**, 183–190.

Biondi F, Qaedan F (2008) A theory-driven approach to tree-ring standardization: defining the biological trend from expected basal area increment. *Tree-Ring Research*, **64**, 81–96.

Borella S, Leuenberger M, Saurer M, Siegwolf R (1998) Reducing uncertainties in $\delta^{13}C$ analysis of tree rings: pooling, milling, and cellulose extraction. *Journal of Geophysical Research*, **103**, 519–526.

Burnham KP, Anderson DR (2002) *Model Selection and Multimodel Inference: A Practical Information-Theoretic Approach*. Springer-Verlag, Heidelberg.

Cabrera M (2001) Evolución de abetares del Pirineo aragonés. *Cuadernos de la Sociedad Española de Ciencias Forestales*, **11**, 43–52.

Camarero JJ, Bigler CJ, Linares JC, Gil-Pelegrín E (2011) Synergistic effects of past historical logging and drought on the decline of Pyrenean silver fir forests. *Forest Ecology and Management*, **262**, 759–769.

Carnicer J, Coll M, Ninyerola M, Pons X, Sánchez G, Peñuelas J (2011) Widespread crown condition decline, food web disruption, and amplified tree mortality with increased climate change-type drought. *Proceedings of the National Academy of Sciences*, **119**, 1515–1525.

Carrer M, Nola P, Motta R, Urbinati C (2010) Contrasting tree-ring growth to climate responses of *Abies alba* toward the southern limit of its distribution area. *Oikos*, **119**, 1515–1525.

Ceulemans R, Mousseau M (1994) Effects of elevated atmospheric CO_2 on woody plants. *New Phytologist*, **127**, 425–446.

Das AJ, Battles JJ, Stephenson NL, van Mantgem PJ (2007) The relationship between tree growth patterns and likelihood of mortality: a study of two tree species in the Sierra Nevada. *Canadian Journal of Forest Research*, **37**, 580–597.

Duquesnay A, Breda N, Stievenard M, Dupouey JL (1998) Changes of tree-ring $\delta^{13}C$ and water-use efficiency of beech (*Fagus sylvatica* L.) in north-eastern France during the past century. *Plant Cell and Environment*, **21**, 565–572.

Farquhar GD, Richards RA (1984) Isotopic composition of plant carbon correlates with water-use efficiency of wheat genotypes. *Australian Journal of Plant Physiology*, **11**, 539–552.

Farquhar GD, O'Leary HM, Berry JA (1982) On the relationship between carbon isotope discrimination and the intercellular carbon dioxide concentration in leaves. *Australian Journal of Plant Physiology*, **9**, 121–137.

Feng X (1998) Long-term C_i/C_a responses of trees in western North America to atmospheric CO_2 concentration derived from carbon isotope chronologies. *Oecologia*, **117**, 19–25.

Ferrio JP, Alonso N, Lopez JB, Araus JL, Voltas J (2006) Carbon isotope composition of fossil charcoal reveals aridity changes in the NW Mediterranean Basin. *Global Change Biology*, **12**, 1253–1266.

Francey RJ (1986) Carbon isotope measurements in baseline air, forest canopy air, and plants. In: *The Changing Carbon Cycle* (eds Trabalka JR, Reichle DE), pp. 160–174. Springer-Verlag, New York.

Fritts HC (1976) *Tree Rings and Climate*. Academic Press, London.

Gagen M, Finsinger W, Wagner-Cremer F *et al.* (2011) Evidence of changing intrinsic water-use efficiency under rising atmospheric CO_2 concentrations in Boreal Fennoscandia from subfossil leaves and tree ring $\delta_{13}C$ ratios. *Global Change Biology*, **17**, 1064–1072.

Galiano L, Martínez-Vilalta J, Lloret F (2011) Carbon reserves and canopy defoliation determine the recovery of Scots pine 4 yr after a drought episode. *New Phytologist*, **190**, 750–759.

Gonzalez P, Neilson RP, Drapek RJ (2010) Global patterns in the vulnerability of ecosystems to vegetation shifts due to climate change. *Global Ecology and Biogeography*, **19**, 755–768.

Heaton THE (1999) Spatial, species, and temporal variations in the $^{13}C/^{12}C$ ratios of C_3 plants: implications for palaeodiet studies. *Journal of Archaeological Science*, **26**, 637–649.

Holmes RL (1983) Computer-assisted quality control in tree-ring dating and measurement. *Tree-Ring Bulletin*, **43**, 68–78.

Huang J-G, Bergeron Y, Denneler B, Berninger F, Tardif J (2007) Response of forest trees to increased atmospheric CO_2. *Critical Reviews in Plant Sciences*, **26**, 265–283.

Hultine KR, Marshall JD (2000) Altitude trends in conifer leaf morphology and stable carbon isotope composition. *Oecologia*, **123**, 32–40.

Hyvönen R, Ågren GI, Linder S *et al.* (2007) The likely impact of elevated CO_2, nitrogen deposition, increased temperature and management on carbon sequestration in temperate and boreal forest ecosystems: a literature review. *New Phytologist*, **173**, 463–480.

Jäggi M, Saurer M, Fuhrer J, Siegwolf R (2002) The relationship between the stable carbon isotope composition of needle bulk material, starch, and tree rings in *Picea abies*. *Oecologia*, **131**, 325–332.

Körner C (2000) Biosphere responses to CO_2 enrichment. *Ecological Applications*, **10**, 1590–1619.

Körner C, Morgan J, Norby R (2007) CO_2 fertilization: when, where, how much? In: *Terrestrial Ecosystems in a Changing World* (eds Canadell J, Pataki DE, Pitelka L), pp. 9–21. Springer-Verlag, Berlin.

Koutavas A (2008) Late 20th century growth acceleration in Greek firs (*Abies cephalonica*) from Cephalonia Island, Greece: a CO_2 fertilization effect? *Dendrochronologia*, **26**, 13–19.

Leavitt SW, Danzer SR (1993) Method for batch processing small wood samples to holocellulose for stable-carbon isotope analysis. *Annals of Chemistry*, **65**, 87–89.

Leavitt SW, Long A (1982) Evidence for $^{13}C/^{12}C$ fractionation between tree leaves and wood. *Nature*, **298**, 742–744.

Leavitt SW, Long A (1986) Stable-carbon isotope variability in tree foliage and wood. *Ecology*, **67**, 1002–1010.

Levanič T, Čater M, McDowell NG (2011) Associations between growth, wood anatomy, carbon isotope discrimination and mortality in a *Quercus robur* forest. *Tree Physiology*, **31**, 298–308, doi: 10.1093/treephys/tpq111.

Linares JC, Tíscar PA (2011) Buffered climate change effects in a Mediterranean pine species: range limit implications from a tree-ring study. *Oecologia*; doi: 10.1007/s00442-011-2012-2.

Linares JC, Delgado-Huertas A, Camarero JJ, Merino J, Carreira JA (2009) Competition and drought limit the water-use efficiency response to rising atmospheric CO_2 in the Mediterranean fir *Abies pinsapo*. *Oecologia*, **161**, 611–624.

Linares JC, Camarero JJ, Carreira JA (2010) Competition modulates the adaptation capacity of forests to climatic stress: insights from recent growth decline and death in relict stands of the Mediterranean fir *Abies pinsapo*. *Journal of Ecology*, **98**, 592–603.

Litton C, Raich JW, Ryan MG (2007) Carbon allocation in forest ecosystems. *Global Change Biology*, **13**, 2089–2109.

Loader NJ, Robertson I, Barker AC, Switsur VR, Waterhouse JS (1997) An improved technique for the batch processing of small whole wood samples to alpha-cellulose. *Chemical Geology*, **136**, 313–317.

Macias M, Andreu L, Bosch O, Camarero JJ, Gutiérrez E (2006) Increasing aridity is enhancing silver fir (*Abies alba* Mill.) water stress in its south-western distribution limit. *Climatic Change*, **79**, 289–313.

Marshall JD, Monserud RA (1996) Homeostatic gas-exchange parameters inferred from $^{13}C/^{12}C$ in tree rings of conifers. *Oecologia*, **105**, 13–21.

Martinez-Vilalta J, López BC, Adell N, Badiella L, Ninyerola M (2008) Twentieth century increase of Scots pine radial growth in NE Spain shows strong climate interactions. *Global Change Biology*, **14**, 2868–2881.

McCarroll D, Loader NJ (2004) Stable isotopes in tree-rings. *Quaternary Science Reviews*, **23**, 771–801.

McDowell N, Pockman WT, Allen CD *et al*. (2008) Mechanisms of plant survival and mortality during drought: why do some plants survive while others succumb to drought? *New Phytologist*, **178**, 719–739.

McDowell N, Allen CD, Marshall L (2010) Growth, carbon-isotope discrimination, and drought-associated mortality across a *Pinus ponderosa* elevational transect. *Global Change Biology*, **16**, 399–415.

Müller EHR, Stierlin HR (1990) *Sanasilva Tree Crown Photos with Percentages of Foliage Loss*. WSL, Birmensdorf.

Niinemets U, Peñuelas J, Flexas J (2011) Evergreens favored by higher responsiveness to increased CO_2. *Trends in Ecology & Evolution*, **26**, 136–142, doi: 10.1016/j.tree.2010.12.012.

Norby RJ, DeLucia EH, Gielen B *et al*. (2005) Forest response to elevated CO_2 is conserved across a broad range of productivity. *Proceedings of the National Academy of Sciences USA*, **102**, 18052–18056.

Nowak RS, Ellsworth DS, Smith SD (2004) Functional responses of plants to elevated atmospheric CO_2 – do photosynthetic and productivity data from FACE experiments support early predictions? *New Phytologist*, **162**, 253–280.

Ogle K, Whitham TG, Cobb NS (2000) Tree-ring variation in pinyon predicts likelihood of death following severe drought. *Ecology*, **81**, 3237–3243.

O'Leary MH (1981) Carbon isotope fractionation in plants. *Phytochemistry*, **20**, 553–567.

Pedersen BS (1998) Modeling tree mortality in response to short and long-term environmental stresses. *Ecological Modelling*, **105**, 347–351.

Peguero-Pina JJ, Camarero JJ, Abadía A, Martín R, González-Cascón R, Morales F, Gil-Pelegrín E (2007) Physiological performance of silver-fir (*Abies alba* Mill.) populations under contrasting climates near the south-western distribution limit of the species. *Flora*, **202**, 226–236.

Peñuelas J, Hunt JM, Ogaya R, Jump AS (2008) Twentieth century changes of tree-ring $\delta^{13}C$ at the southern range-edge of *Fagus sylvatica*: increasing water-use efficiency does not avoid the growth decline induced by warming at low altitudes. *Global Change Biology*, **14**, 1–13.

Peñuelas J, Canadell J, Ogaya R (2010) Increased water-use efficiency during the 20th century did not translate into enhanced tree growth. *Global Ecology and Biogeography*, **20**, 597–608.

Pinheiro J, Bates D, DebRoy S, Sarkar D (2011) *nlme: Linear and Nonlinear Mixed Effects Models. R Package Version 3.1-92*. Available at: http://cran.r-project.org/web/packages/nlme/index.html (accessed 22 April 2011).

Poorter H, Navas ML (2003) Plant growth and competition at elevated CO_2: on winners, losers and functional groups. *New Phytologist*, **157**, 175–198.

Poorter H, Pérez-Soba M (2001) The growth response of plants to elevated CO_2 under non-optimal environmental conditions. *Oecologia*, **129**, 1–20.

R Development Core Team (2011) *R: A Language and Environment for Statistical Computing*. R Foundation for Statistical Computing, Vienna. Available at: http://www.r-project.org/(accessed 22 April 2011).

Robertson I, Leavitt SW, Loader NJ, Buhay B (2008) Progress in isotope dendroclimatology. *Chemical Geology*, **252**, EX1–EX4.

Sala A, Piper F, Hoch G (2010) Physiological mechanisms of drought-induced tree mortality are far from being resolved. *New Phytologist*, **186**, 274–281.

Saurer M, Siegwolf R, Schweingruber F (2004) Carbon isotope discrimination indicates improving water-use efficiency of trees in northern Eurasia over the last 100 years. *Global Change Biology*, **10**, 2109–2120.

Seibt U, Rajabi A, Griffiths H, Berry JA (2008) Carbon isotopes and water use efficiency – sense and sensitivity. *Oecologia*, **155**, 441–454.

Silva LCR, Anand M, Leithead MD (2010) Recent widespread tree growth decline despite increasing atmospheric CO_2. *PLoS ONE*, **5**, article number: e11543.

Sitch S, Huntingford C, Gedney N *et al*. (2008) Evaluation of the terrestrial carbon cycle, future plant geography and climate-carbon cycle feedbacks using five dynamic global vegetation models (DGVMs). *Global Change Biology*, **14**, 2015–2039.

Suarez ML, Ghermandi L, Kitzberger T (2004) Factors predisposing episodic drought-induced tree mortality in *Nothofagus* – site, climatic sensitivity and growth trends. *Journal of Ecology*, **92**, 954–966.

Tardif J, Camarero JJ, Ribas M, Gutiérrez E (2003) Spatiotemporal variability in tree ring growth in the Central Pyrenees: climatic and site influences. *Ecological Monographs*, **73**, 241–257.

Thuiller W, Albert C, Araújo MB *et al*. (2008) Predicting global change impacts on plant species' distributions: future challenges. *Perspectives in Plant Ecology, Evolution and Systematics*, **9**, 137–152.

Waring RH, Landsberg JJ, Williams M (1998) Net primary production of forests: a constant fraction of gross primary production? *Tree Physiology*, **18**, 129–134.

Waterhouse JS, Switsur VR, Barker AC, Carter AHC, Hemming DL, Loader NJ, Robertson I (2004) Northern European trees show a progressively diminishing response to increasing atmospheric carbon dioxide concentrations. *Quaternary Science Reviews*, **23**, 803–810.

Wullschleger SD, Tschaplinski TJ, Norby RJ (2002) Plant water relations at elevated CO_2 implications for water-limited environments. *Plant Cell and Environment*, **25**, 319–331.

Zar JH (1999) *Biostatistical Analysis*. Prentice Hall, Upper Saddle River, New Jersey.

Zuur AF, Ieno EN, Walker N, Saveliev AA, Smith GM (2009) *Mixed Effects Models and Extensions in Ecology with R*. Springer, New York.

Supporting Information

Additional Supporting Information may be found in the online version of this article:

Figure S1. Landscape view of the nondeclining Gamueta (GA; see Table 1) site (42°53′N, 0°48′W, elevation: 1400 m). No *Abies alba* (dark-green crowns) defoliation was detected at this site. The light-green and deciduous crowns correspond to *Fagus sylvatica*.

Figure S2. Landscape view of the declining Paco Ezpela-high (PE; see Table 1) site (42°45′N, 0°52′W, elevation: 1232 m). This declining site was one of the most heavily affected stands, with 50% of all sampled trees showing severe defoliation. Red and defoliated crowns correspond to declining trees, whereas light-green crowns correspond to *F. sylvatica*.

Figure S3. Estimation of ambient CO2 partial pressure from values of *Ca* mole fraction (a) mean May–August air temperature (b) and total barometric pressure (c) Ambient CO_2 partial pressure (d) was computed for declining and nondeclining sites, respectively.

Figure S4. Theoretical scenarios for the regulation of plant-gas exchange fractionation during CO_2 diffusion through the stomata. (a) Isotopic composition of atmospheric CO2 ($\Delta 13Ca$, upper graph) and isotope values of tree rings corresponding to the three scenarios ($\Delta 13C$ in tree rings, lower graphs). The discrimination Δ is also indicated. (b) *Ci*/*Ca* (axis to the left) and Δ (axis to the right), (c) *Ci*-*Ca* (axis to the left) and intrinsic water-use efficiency (iWUE, right axis), (d) *Ca* and *Ci*.

Table S1. Characteristics of the meteorological stations used to describe climatic conditions in declining and nondeclining *Abies alba* sites.

Please note: Wiley-Blackwell are not responsible for the content or functionality of any supporting materials supplied by the authors. Any queries (other than missing material) should be directed to the corresponding author for the article.